Heat-shock protein 27 (Hsp27) as a target of methylglyoxal in gastrointestinal cancer

Tomoko Oya-Ito [a,b,*], Yuji Naito [b], Tomohisa Takagi [b], Osamu Handa [b], Hirofumi Matsui [c], Masaki Yamada [d], Keisuke Shima [d], Toshikazu Yoshikawa [a,b]

[a] Department of Medical Proteomics, Kyoto Prefectural University of Medicine, 465 Kaji-i, Kyoto 602-8566, Japan
[b] Department of Molecular Gastroenterology and Hepatology, Graduate School of Medical Science, Kyoto Prefectural University of Medicine, 465 Kaji-i, Kyoto 602-8566, Japan
[c] Division of Gastroenterology, Graduate School of Comprehensive Human Sciences, University of Tsukuba, 1-1-1 Ten-nodai, Tsukuba 305-8575, Japan
[d] Shimadzu Corporation, 1 Nishinokyo-kuwahara, Kyoto 604-8511, Japan

ARTICLE INFO

ABSTRACT

The molecular mechanisms underlying the posttranslational modification of proteins in gastrointestinal cancer are still unknown. Here, we investigated the role of methylglyoxal modifications in gastrointestinal tumors. Methylglyoxal is a reactive dicarbonyl compound produced from cellular glycolytic intermediates that reacts non-enzymatically with proteins. By using a monoclonal antibody to methylglyoxal-modified proteins, we found that murine heat-shock protein 25 and human heat-shock protein 27 were the major adducted proteins in rat gastric carcinoma mucosal cell line and human colon cancer cell line, respectively. Furthermore, we found that heat-shock protein 27 was modified by methylglyoxal in ascending colon and rectum of patients with cancer. However, methylglyoxal-modified heat-shock protein 25/heat-shock protein 27 was not detected in non cancerous cell lines or in normal subject. Matrix-associated laser desorption/ ionization mass spectrometry/mass spectrometry analysis of peptide fragments identified Arg-75, Arg-79, Arg-89, Arg-94, Arg-127, Arg-136, Arg-140, Arg-188, and Lys-123 as methylglyoxal modification sites in heat-shock protein 27 and in phosphorylated heat-shock protein 27. The transfer of methylglyoxal-modified heat-shock protein 27 into rat intestinal epithelial cell line RIE was even more effective in preventing apoptotic cell death than that of native control heat-shock protein 27. Furthermore, methylglyoxal modification of heat-shock protein 27 protected the cells against both the hydrogen peroxide- and cytochrome c-mediated caspase activation, and the hydrogen peroxide-induced production of intracellular reactive oxygen species. The levels of lactate converted from methylglyoxal were increased in carcinoma mucosal cell lines. Our results suggest that posttranslational modification of heat-shock protein 27 by methylglyoxal may have important implications for epithelial cell injury in gastrointestinal cancer.

© 2011 Elsevier B.V. All rights reserved.

1. Introduction

Most cancer cells produce energy by glycolysis rather than oxidative phosphorylation via the tricarboxylic acid (TCA) cycle, even in the presence of an adequate oxygen supply (Warburg effect) [1]. Extremely low glucose, coupled with high lactate and glycolytic intermediate concentrations, were found in tumor tissues obtained from 16 colon and 12 stomach cancer patients, indicating enhanced glycolysis, and thus confirming the Warburg effect [2]. Methylglyoxal

(MG) modifies tissue proteins via the Maillard reaction, and in the glycolytic pathway, resulting in advanced glycation end products (AGEs) that can alter protein structure and function. In human non-small-cell lung cancer tissues, the AGEs Nε-(carboxymethyl) lysine (CML) and argpyrimidine have been detected by immunohistochemistry [3].

Small heat-shock proteins, including murine heat-shock protein 25 (Hsp25) which is the murine homolog of human heat-shock protein 27 (Hsp27), human Hsp27, and alpha B-crystallin, are molecular chaperones constitutively expressed in several mammalian cells, particularly in pathological conditions [4]. Short-chain fatty acids, such as butyrate, induce a time- and concentration-dependent increase in Hsp25 protein expression in rat intestinal epithelial cells [5]. Small heat-shock proteins share functions as diverse as protection against toxicity mediated by aberrantly folded proteins, and oxidative-inflammation conditions [4,6]. In addition, these proteins share anti-apoptotic properties and are tumorigenic when expressed in cancer cells [4]. Hsp27 is phosphorylated at serines 15, 78 and 82 by mitogen-activated protein kinase associated protein kinases 2 and 3

(MAPKAP kinases 2 and 3), which are themselves activated by phosphorylation by MAP p38 protein kinase [7,8]. However, the mechanism regulating Hsp27 action in cancer cells is still unknown. In a previous study, we showed that Hsp27 has enhanced anti-apoptotic properties after MG modification in lens epithelial cells [9]. Here, we examine the effect of MG modification on the anti-apoptotic function of Hsp27 in rat intestinal epithelial cell line.

2. Materials and methods

2.1. Reagents and cell culture

Human Hsp27 polyclonal and mouse Hsp25 polyclonal antibodies were obtained from StressGen Biotechnologies Corp. (Victoria, British Columbia, Canada). Human phosho-Hsp27 (Ser-82) polyclonal and human Hsp27 monoclonal antibodies were obtained from Cell Signaling Technology Japan, K.K. (Tokyo, Japan). Horseradish peroxidase (HRP)-linked anti-rabbit IgG was obtained from Cell Signaling Technology, Inc. (Beverly, MA, United States). HRP-linked anti-mouse IgG, Deep Purple Total Protein Stain, Protein A Sepharose and enhanced chemiluminescence (ECL) Plus Western blotting detection reagents were obtained from GE Healthcare UK Ltd. (Buckinghamshire, England). *Staphylococcus aureus* V8 protease (endoproteinase Glu-C) was obtained from Wako Pure Chemical Industries, Ltd. (Osaka, Japan). D-Lactic acid, L-lactic acid, D-lactate dehydrogenase (D-LDH) (*Lactobacillus leichmannii*), L-lactate dehydrogenase (L-LDH) (bovine heart), glutamate-pyruvate transamirase, NAD^+ and pyruvate were purchased from J.K. International Inc. (Tokyo, Japan). Normal rat gastric mucosal cell line RGM-1 and rat gastric carcinoma mucosal cell line RGK-1 [10] were donated by Dr. Hirofumi Matsui of the University of Tsukuba, Japan. RGM-1 cells, RGK-1 cells, human colon cancer cell line HT-29, and rat intestinal epithelial cell line RIE were grown in a 1:1 mixture of Dulbecco's modified Eagle medium and Ham's F-12 medium (DMEM/F12; Cosmo Bio, Tokyo, Japan) supplemented with 10% fetal calf serum (FCS; Gibco, Grand Island, NY, United States). Young adult mouse colon (YAMC) epithelial cells were grown in RPMI with 5% fetal calf serum, 100 ng/μl IFN-γ, 2 mM glutamine, 50 μg/ml gentamicin, 100 U/ml penicillin, 100 μg/ml streptomycin, and 1× insulin/transferrin/selenium. All cells were grown at 37 °C in a humidified 5% CO_2 atmosphere.

2.2. Sample preparation

Cells were harvested by centrifugation, rinsed in phosphate-buffered saline (PBS), and resuspended in homogenization buffer (8 M Urea, 4% 3-[(3-cholamidopropyl)dimethylammonio]-1-propanesulfonic acid (CHAPS), 40 mM Tris) containing nuclease and protein inhibitors (GE Healthcare UK Ltd.) at a volume approximately equal to that of the packed cells. The suspension was transferred to an ultracentrifuge tube and the nuclei were removed by centrifugation (20 min at 20,000g, 25 °C). Lysates were precipitated using the Plus One 2D Clean-up kit as recommended by the manufacturer (GE Healthcare UK Ltd.). The protein concentration in the supernatant fraction was determined using the Bradford assay, with bovine serum albumin as the standard. Samples were solubilized in 8 M urea, 2% CHAPS, 20 mM dithiothreitol (DTT), 0.5% ZOOM Carrier Ampholytes 3–10 (Invitrogen Japan K.K., Tokyo, Japan), and 0.002% bromophenol blue. Protein lysates (50 μg) were separated on two-dimensional PAGE gels. IPG strips, pH 3–10 NL or pH 4–7 (Invitrogen Japan K.K.), were rehydrated overnight with the protein samples. Proteins were separated based on their isoelectric point by IEF using the ZOOM IPG Runner (Invitrogen Japan K.K.) with a maximal voltage of 2000 V and 50 μA per gel. Following IEF, IPG strips were incubated in equilibration buffer I (6 M urea, 130 mM dithiothreitol, 30% glycerol, 45 mM Tris base, 1.6% LDS, 0.002% bromophenol blue; Genomic Solutions) and once in equilibration buffer II (6 M urea, 135 mM iodoacetamide, 30%

glycerol, 45 mM Tris base, 1.6% LDS, 0.002% bromophenol blue; Genomic Solutions) for 15 min each. Equilibrated IPG strips were applied to 4–12% Bis–Tris gradient gels (Invitrogen Japan K.K.), and the proteins were separated in the second dimension based on their molecular size using NuPAGE MOPS buffer (Invitrogen Japan K.K.) at 200 V for 55 min. Following electrophoresis, gels were transferred onto nitrocellulose and immunoblotted with the relevant antibodies. The blots were probed with anti-argpyrimidine monoclonal antibody (mAb6B), a kind gift from Prof. Koji Uchida (Nagoya University, Japan), diluted 1:5000 in 0.1% (v/v) tween 20 blocking solution in TBS for 2.5 h at room temperature. Immunoreactivity was detected using an HRP-labeled secondary antibody with an ECL Plus Western blotting detection reagents system. Each immunoblot was repeated three times from independent experiments.

2.3. Immunoprecipitation

Cells were washed, collected, and resuspended in PBS. Cells were pelleted by centrifugation and lysed in immunoprecipitation buffer (Tris–HCl, pH 7.6, 150–400 mm NaCl, and 1% Nonidet P-40, 1 mm EDTA, and protein inhibitors). The lysates were cleared by centrifugation and were precleared by a 1-h incubation with 20 μl of a 50% slurry of Protein A Sepharose Fast Flow (GE Healthcare UK Ltd.). The cleared lysates were then incubated overnight with Hsp27 or Hsp25 polyclonal antibodies. Human Hsp27 polyclonal and mouse Hsp25 polyclonal antibodies detect endogenous levels of total human Hsp27 protein and mouse and rat Hsp25 protein, respectively. These antibodies do not cross-react with other heat-shock proteins. The antibody-captured complexes were recovered with fresh Protein A Sepharose Fast Flow beads (20 μl of original bead slurry/sample) by incubation with lysate/antibody mixture at 4 °C for 2 h. The beads were then washed three times with the immunoprecipitation buffer. SDS Laemmli buffer was added to the beads, and the beads were boiled to elute the proteins. After centrifugation, the immunoprecipitated eluted proteins from the beads were subjected to SDS–PAGE and Western blotting.

2.4. Tissue samples

MG modification of Hsp27 was determined by immunoprecipitation and Western blot analysis in ascending colon and rectum of 6 patients. This study was approved by the Ethics Committee of Kyoto Prefectural University of Medicine (Kyoto, Japan) and informed consent was obtained from all participants prior to enrollment. Six specimens from patients (2 males and 4 females) with a mean age of 76 ± 3 (range 73–80) years were clinically and pathologically examined and diagnosed as adenoma and advanced cancer. The tissue samples were immediately frozen in liquid nitrogen and stored at −80 °C until use.

2.5. Proteomics of MG-modified Hsp27

Recombinant human Hsp27 (0.1 mg/ml) was incubated with various concentrations of MG in 50 mM phosphate buffer (pH 7.4) at 37 °C for 24 h. The monomers of native control Hsp27 and MG-modified Hsp27 picked from the gels were rehydrated on ice for 45 min in 50 mM ammonium bicarbonate containing 12.5 μg/μl sequencing grade modified trypsin (Promega, Madison, WI). Digestion was carried out at 37 °C for 15 h. The resulting peptides were sequentially extracted for 20 min each in 50-μl aliquots of 20 mM ammonium bicarbonate followed by 1% trifluoroacetic acid, 0.1% trifluoroacetic acid in 50% acetonitrile and, finally, 5% acetic acid in 50% acetonitrile. Combined extracts were concentrated in a Speed Vac to ~5 μl, re-dissolved in 45 μl of 0.1 M acetic acid, and centrifuged for 2 min at 14,000g. The supernatant fractions were carefully transferred into a fresh tube and concentrated to ~5 μl. After evaporation, the

digests were analyzed by matrix-associated laser desorption/ioniza-tion mass spectrometry (MALDI-MS). MS analysis was performed using an AXIMA Performance MALDI-TOF/TOF mass spectrometer (Shimadzu Co., Kyoto, Japan), and alpha-cyano-4-hydroxycinnamic acid (CHCA) solution was used as the MALDI matrix. MS/MS analysis was performed using an AXIMA Resonance MALDI-QIT TOF mass spectrometer (Shimadzu Co.), and 2,5-dihydroxybenzoic acid (DHB) solution was used as the MALDI matrix. On the other hand, prior to MS/MS analysis, the low molecular weight reactants were removed from the crude reaction mixture containing MG and Hsp27 by centrifugal filtration (molecular weight cut-off of 10,000, Millipore). Hsp27 and MG-modified Hsp27 (25 μg) were digested with trypsin in 0.2 ml of 100 mM Tris–HCl buffer (pH 8.0) at 37 °C for 24 h using an enzyme:substrate ratio of 1:50 (w/w), followed by V8 protease in Tris–HCl buffer (pH 7.8) at 37 °C for 18 h using an enzyme:substrate ratio of 1:50 (w/w). The resulting peptides were analyzed by LC-MALDI-TOF MS/MS using a Prominence nanoLC system and an AXIMA-Performance MALDI-TOF/TOF mass spectrometer (Shimadzu Co.). CHCA was used as the matrix.

2.6. Treatment of Hsp27 with BioPORTER

MG (0.5 mM)-modified, or native control Hsp27, was treated with BioPORTER according to the manufacturer's instructions (Gene Therapy Systems, Inc., San Diego, CA). Briefly, the BioPORTER reagent was suspended in methanol and 15 μl aliquots were air dried in 0.5 ml Eppendorf tubes. One hundred microliters of PBS, containing 7.5 μg of protein was added to each tube, thoroughly mixed by vortexing for 15 s, and then incubated at room temperature for 5 min. RIE cells in DMEM/F12 containing 10% FCS were cultured in six-well plates. When cells reached 80% confluence, the adherent cells were transferred into new plates containing one of the following: BioPORTER alone, BioPORTER with 7.5 μg of native control Hsp27, or BioPORTER with 7.5 μg of MG-modified Hsp27, in serum-free DMEM/F12. Cells were incubated for 4 h at 37 °C in a humidified 5% CO_2 atmosphere, and then washed with PBS. Introduced native control Hsp27 and MG-modified Hsp27 were quantitated by densitometric analysis of Western blots using CS Analyzer—Image Analysis Software (ATTO Corporation, Tokyo). Protein loading in all of the experiments was normalized by stripping the blots and then reprobing with anti-tubulin antibody. The ratio of introduced Hsp27 protein band density to tubulin band density was calculated. Three independent experiments were performed.

2.7. Assay of cell viability

After the introduction of native control Hsp27 and MG-modified Hsp27 (MG-Hsp27) using BioPORTER, the cell viability was measured using the 2-(2-methoxy-4-nitrophenyl)-3-(4-nitrophenyl)-5-(2,4-disulfophenyl)-2H-tetrazolium, monosodium salt (WST-8) in Cell Counting Kit-8 (Wako Pure Chemical Industries, Ltd.). In brief, treated RIE cells were cultured in 96-well plates for 24 and 48 h, followed by incubation with WST-8 for 4 h. Absorbance was measured at 450 nm, and cell viability was determined by comparing the ratio of absorbance for each experiment to that for the control experiments.

2.8. Apoptosis

To detect apoptotic cells, RIE cells were treated with hydrogen peroxide and then labeled with annexin V-FITC and propidium iodide (PI) for 15 min. Fluorescent cells were detected using FACSCalibur and analyzed using the CellQuest analysis program (BD Biosciences, Tokyo, Japan). For measurement of reactive oxygen species (ROS) generation, RIE cells were incubated with aminophenyl fluorescein (APF), 2-[6-(4′-amino) phenoxy-3H-xanthen-3-on-9-yl] benzoic acid (Invitrogen Japan K.K.), for 30 min, and then treated with hydrogen

peroxide. The cells were scraped from the culture dishes, and dispersed by pipetting as gently as possible to avoid mechanical damage. Fluorescence intensity was measured using a microtiter plate reader (SpectraMax M2/M2e, Molecular Devices Corp. Tokyo, JAPAN), with an excitation wavelength of 488 nm and an emission wavelength of 515 nm. Data were expressed as mean ± SEM of three independent measurements.

2.9. Activation of caspase-3 and caspase-9

Nuclei-free, mitochondria-free cytosolic extracts were prepared as previously described [9]. Cell-free extracts (100 μg) derived from Hsp27-introduced cells were incubated with 10 μM cytochrome c from bovine heart (Sigma) and 1 mM dATP (Sigma) for 30 min. These extracts were then incubated with 20 mM DEVD-AFC, or LEHD-AFC (Calbiochem, San Diego, CA), at 37 °C for 90 min. Protein lysates (200 μg) were incubated with 1.0 mM DEVD-AFC or LEHD-AFC at 37 °C for 90 min after apoptosis induction by treatment with hydrogen peroxide. AFC released from the substrates was measured using a microtiter plate reader with an excitation wavelength of 400 nm and an emission wavelength of 505 nm. Data were expressed as mean ± SEM of three independent measurements.

2.10. Measurement of L-lactate and D-lactate

The determination of D-lactate and L-lactate in RGM-1 and RGK-1 cells was performed by an enzymatic method based on the oxidation of L-lactate and D-lactate to pyruvate by NAD in the presence of L-LDH or D-LDH [11]. According to an instruction, in order to inactivate LDH, cell lysates were heated at 80 °C for 15 min.

2.11. Statistical analysis

All values are expressed as means ± SEM. The data were compared using one-way analysis of variance (ANOVA) followed by Bonferroni's Multiple Comparison Test. p-Values < 0.05 were considered statisti-cally significant.

3. Results

3.1. MG-modified protein in gastrointestinal cancer cells

To search for protein modifications by MG, we used a proteomic approach using two-dimensional (2D) gel electrophoresis and mass spectrometry (MS) in rat gastric mucosal cell line RGM-1 and in rat gastric mucosal carcinoma cell line RGK-1. RGK-1 cells are an N-methyl-N′-nitro-N-nitrosoguanidine (MNNG)-induced mutant of RGM-1 gastric epithelial cell line [10]. The mutant RGK-1 cell line form tumors in all the mice injected after 3 weeks [10]. Whole protein extracts from both RGM-1 and RGK-1 cells were separated by 2D electrophoresis, followed by immunoblot analysis with an anti-MG-modified protein monoclonal antibody. The monoclonal antibody against MG-modified protein specifically recognizes argpyrimidine [12]. A large variety of proteins were stained with an anti-argpyrimidine antibody (Fig. 1A and D) because of endogenous MG modification derived from glycolysis. However, only in RGK-1 cells but not in RGM-1 cells the immunoreactivity of a ~25 kDa protein was identified by an antibody to argpyrimidine, as indicated by arrow (Fig. 1D). It was expected that Hsp25 was modified by MG. Hsp25 in the protein extracts obtained from RGM-1 and RGK-1 cells, was confirmed by immunoblotting using an anti-Hsp25 polyclonal antibody (Fig. 1B and E). This anti-Hsp25 polyclonal antibody has been shown to react with both the phosphorylated and the non-phosphorylated forms of Hsp25 [13,14]. Hsp25 underwent various post-translational modifications including phosphorylation, as shown in Fig. 1B and E. The antibody against phosphorylated Hsp25/Hsp27
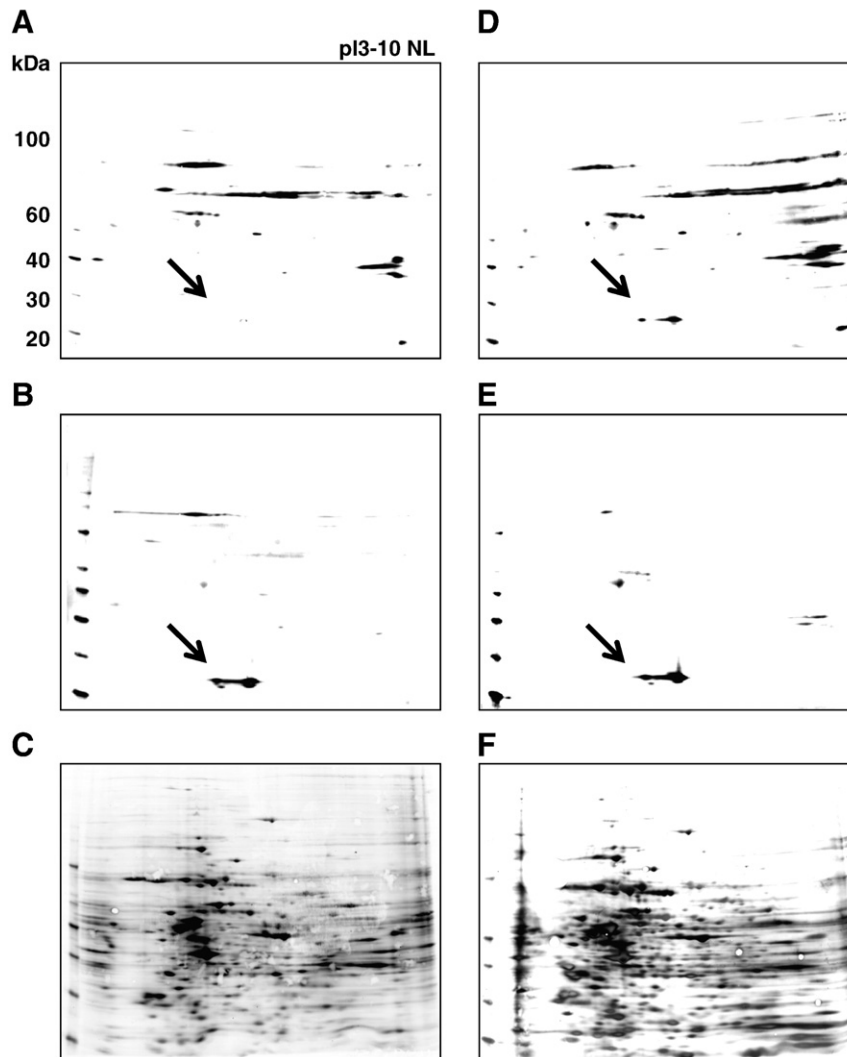
Fig. 1. Two-dimensional electrophoresis and Western blot analysis of proteins obtained from RGM-1 cells and RGK-1 cells. Whole cell extracts from RGM-1 cells (A–C) and RGK-1 cells (D–F) were separated by two-dimensional electrophoresis. MG-modified proteins were identified by immunoblot analysis using an anti-argpyrimidine antibody (A and D). Hsp25 (indicated by arrows) was identified by immunoblotting using an anti-Hsp25 antibody (B and E). Total protein was stained with Deep Purple Total Protein Stain (C and F).

(Ser82) reacted a large number of spots in 2D-PAGE followed by Western blot analyses of RGM-1 cells and RGK-cells (data not shown). This phosphorylated Hsp25/Hsp27 (Ser82) antibody detects endogenous Hsp25/Hsp27 only when phosphorylated at serine 82. The antibody does not recognize other heat-shock proteins such as Hsp70 and Hsp90. Taken together, these results suggest that Hsp25 was phosphorylated in both RGM-1 and RGK-1 cells, and was modified by MG only in mutant RGK-1 cells but not in RGM-1 cells. In Fig. 2H, Hsp25 expression levels were confirmed by Western blot analysis. The same level of Hsp25 expression was observed in RGM-1 and RGK-1 cells. The modification of Hsp25 with MG was verified by immunoprecipitation study (Fig. 2Ha). Immunoprecipitated Hsp25 from mutant RGK-1 cells was recognized by argpyrimidine antibody. These findings were supported by immunoblot analysis in human colon cancer cell line HT-29. Hsp27 (apparent molecular mass, 27 kDa) is the human homolog of rodent protein Hsp25 [15]. The modification of Hsp27 by MG was seen in HT-29 cells (Fig. 2A, B and H). In addition, by using polyclonal antibody against phosphorylated Hsp25/Hsp27 (Ser82) which is produced by immunizing animals with a synthetic phospho-peptide corresponding to residues surrounding Ser82 of human Hsp27, phosphorylation of Hsp27 was also seen in HT-29 cells (Fig. 2C). Oligomerized Hsp27 (approximately 55 kDa) was also detected and this oligomer was both phosphorylated

and MG-modified, as indicated by arrowhead (Fig. 2A, B and C). On the other hand, Hsp25 in rat intestinal epithelial cell line RIE, which was forcibly expressed by treatment with butyrate, was not modified by MG (Fig. 2D and E). Moreover, young adult mouse colon epithelial cell line YAMC showed no modification of Hsp25 by MG (Fig. 2F and G). RIE cells and YAMC cells do not express Hsp25 protein, but short-chain fatty acids such as butyrate, propionate, and acetate in colonic fluid, are the major anions inducing a dose- and time-dependent increase in Hsp25 expression [5]. These findings were confirmed by immunoprecipitation assay using anti-rat Hsp25 polyclonal antibody which recognizes also mouse, bovine, dog, guinea pig and hamster Hsp25. Immunoprecipitated Hsp25 from the RIE cells and the YAMC cells were verified by using anti-Hsp25 monoclonal antibody and did not show immunoreactivity to anti-argpyrimidine monoclonal antibody (Fig. 2Ha and b). Thus, immunoprecipitation studies revealed that MG modifications of both Hsp25 in RGK-1 cells and Hsp27 in HT-29 cells are specific. Furthermore, in the ascending colon and rectum of patients with cancer Hsp27 was modified by MG. Immunoprecipitated Hsp27 with polyclonal antibody from ascending colon and rectum of patient with adenoma and advanced cancer showed cross-reactivity with anti-argpyrimidine monoclonal antibody, whereas that from normal subject showed no reactivity (Fig. 2Ha). The levels of endogenous Hsp27 were confirmed by using monoclonal antibody
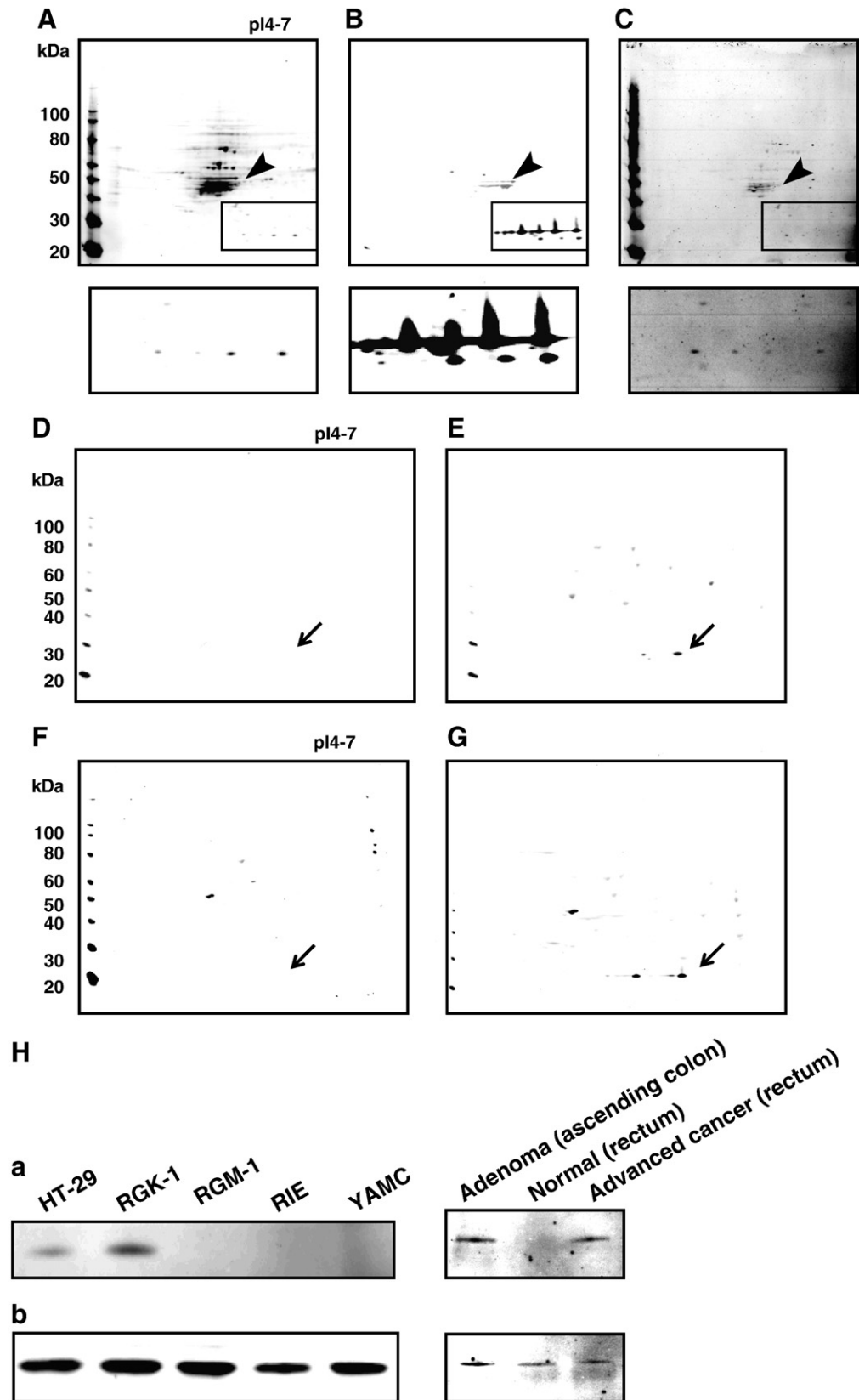
Fig. 2. Detections of MG-modified proteins and Hsp25/Hsp27. Whole cell extracts from HT-29 cells (A–C), RIE cells (D and E), and YAMC cells (F and G) were separated by two-dimensional electrophoresis. MG-modified proteins were identified by immunoblot analysis using anti-argpyrimidine (A, D, and F). Hsp27 (B) and phosphorylated Hsp27 (C) were identified by immunoblot analysis using anti-Hsp27 and anti-pHsp27 (Ser-82), respectively. Forced expression of Hsp25 in RIE cells (D and E) and in YAMC cells (F and G) were induced by treatment with butyrate. Hsp25 (indicated by arrows) was identified by immunoblot analysis using an anti-Hsp25 antibody (E and G). MG modifications of Hsp25/Hsp27 were confirmed by immunoprecipitation assays with Hsp25/Hsp27 and argpyrimidine specific antibodies (H). MG modification in immunoprecipitated Hsp25/Hsp27 from whole cell extracts and from tissue extracts were identified by immunoblot analysis using anti-argpyrimidine antibody (a). The immunoprecipitated Hsp25/27 were verified by immunoblot analyses using anti-Hsp25 antibody (RGM-1, RGK-1, RIE, and YAMC cells) and anti-Hsp27 antibody (HT-29 cells and tissue of patients) (b).

against Hsp27. There was no difference in immunoprecipitated endogenous Hsp27 between cancer and normal. These results suggest that MG modification of Hsp25/Hsp27 contributes to the altered metabolism of cancer. The expression level of Hsp25/Hsp27 was not involved in the pathogenesis of cancer.

3.2. MG modification sites on Hsp27

To identify MG modification sites, human recombinant Hsp27 was incubated with MG. Incubation of Hsp27 (0.1 mg/ml) and phosphorylated Hsp27 (pHsp27, 0.1 mg/ml) with up to 5 mM MG in 50 mM sodium phosphate buffer (pH 7.4) at 37 °C, resulted in a concentration-dependent polymerization, which was associated with the covalent binding of MG to protein (Fig. 3). Moreover, immunoreactivity with the anti-argpyrimidine monoclonal antibody (mAb6B) was observed in polymerized Hsp27. Native Hsp27 was more easily polymerized by MG than phosphorylated Hsp27. To identify the MG modification sites on Hsp27, monomers of both the native and MG-treated Hsp27 in the gels were digested with trypsin. The resulting peptides were subjected to matrix-assisted laser desorption/ionization mass spectrometry (MALDI-MS). Sequence coverage of both the native, and MG-modified Hsp27 (MG-Hsp27) was 67% and 63%, respectively. The MALDI-TOF MS spectra generated from native Hsp27 and MG-Hsp27 are shown in Fig. 4A. To confirm the MG modification sites, the MG-modified fragments were also analyzed using a MALDI-QIT TOF mass spectrometer. The MS/MS spectrum of the $[M+H]^+$ ion at m/z 2882.5 from the MG-modified fragment with the sequence LATQSNEITIPVTFESRAQLGGPEAAK, plus the mass addition of 54 Da, is shown in Fig. 4B. In the MS/MS analysis, the singly charged C-terminal product ions (y12–y13, y15, y17–y20, and y23) and the lysine loss ions (y12-K and y17-K) were seen. The singly

charged N-terminal product ions (b20, b22, and b24–b26) were also observed, suggesting that the MG modification site in this sequence is on Arg-188. This technique identified eleven peptides, which contained MG adducts at Arg-136, Arg-188, and Lys-123. The peptides identified by MALDI analysis of enzymatic digests of MG-Hsp27 are listed in Table 1. These results suggest that 5-hydro-5-methylimdazolone, and carboxyethyllysine, are generated by MG modification of Hsp27.

To characterize the formation of argpyrimidine in MG-Hsp27, MG-treated Hsp27 was digested with trypsin and V8 protease, and then analyzed by LC-MALDI-TOF MS/MS. The sequence coverage of MG-Hsp27 was 93%. The MS/MS spectrum of the $[M+H]^+$ ion at m/z 1377.4 from the MG-modified fragment with the sequence HGYISRCFTR, plus the mass addition of 80 Da, is shown in Fig. 4C. The singly charged N-terminal product ions (b1–b9), and the singly charged C-terminal product ions (y1–y10), were observed. Fig. 4D shows the MS/MS spectrum of the $[M+H]^+$ ion at m/z 1265.3 with the sequence SRAQLGGPEAAK, plus the mass addition of 80 Da. In the MS/MS analysis, single charged product ions (b1–b12 and y1–y12) were observed. These data indicate that both Arg-136 and Arg-188 represent the MG modification sites due to the 80 Da increase in the mass value, and are due to argpyrimidine modification. Peptides identified by LC-MALDI analysis of the enzymatic digests of MG-Hsp27 are listed in Table 1. This technique identified eleven peptides, which contained MG adducts at Arg-5, Arg-37, Arg-56, Arg-75, Arg-79, Arg-89, Arg-94, Arg-96, Arg-127, Arg-136, Arg-140, and Arg-188. These results suggest that 5-hydro-5-methylimdazolone is associated with Arg-5, Arg-37, Arg-56, Arg-75, Arg-79, Arg-89, Arg-94, Arg-96, Arg-127, Arg-136, Arg-140, and Arg-188. Moreover, dihydroxyimidazolidine appears to associate with Arg-188.

The peptides identified by LC-MALDI analysis of enzymatic digests of MG-modified phosphorylated Hsp27 (MG-pHsp27) are listed in Table 2. Sequence coverage of MG-pHsp27 digested with both trypsin and V8 protease was 72%. The MS/MS analyses showed that Hsp27 was phosphorylated, and 5-hydro-5-methylimdazolone, dihydroxyimidazolidine, and carboxyethyllysine were generated by MG modification of phosphorylated Hsp27. This technique identified 18 peptides, which contained MG adducts at Arg-75, Arg-89, Arg-94, Arg-127, Arg-136, Arg-140, Arg-188, Lys-114 and Lys-123. 5-Hydro-5-methylimdazolone was associated with Arg-75, Arg-89, Arg-94, Arg-127, Arg-136, Arg-140, and Arg-188. Dihydroxyimidazolidine was generated at Arg-75 and Arg-188. The association of argpyrimidine with pHsp27 was not detected.

To verify that recombinant Hsp27 reflects the situation in vivo, MG-Hsp27 and MG-pHsp27 were analyzed by 2D-PAGE followed by Western blotting, and compared to Hsp27 both in HT-29 cells and in inflamed mucosa of patient obtained from colonic biopsy (unpublished data). It was difficult to detect MG-Hsp27 in the ascending colon and rectum of patients with cancer by 2D-PAGE followed by Western blotting because of low protein concentrations. The results of recombinant MG-Hsp27 and MG-pHsp27 were similar to those in HT-29 cells. Recombinant MG-Hsp27 was detected as polymerized and migrated toward a more acidic pI form by 2D-PAGE. Recombinant MG-pHsp27 was mainly detected around 25 kDa and 55 kDa. Both recombinant MG-Hsp27 and MG-pHsp27 protein spots were also detected as same positions as those from inflamed mucosa (unpublished data).

3.3. Effect of MG modification on apoptosis

It is known that Hsp27 prevents apoptosis [16]. To investigate the effect of MG modification on the anti-apoptotic properties of Hsp27, we compared the protective effects of native unmodified Hsp27, and MG-Hsp27, against hydrogen peroxide-induced apoptosis in RIE cells. RIE cells do not express Hsp27 protein. Native Hsp27 and MG-Hsp27 were introduced into RIE cells using the BioPORTER reagent, which
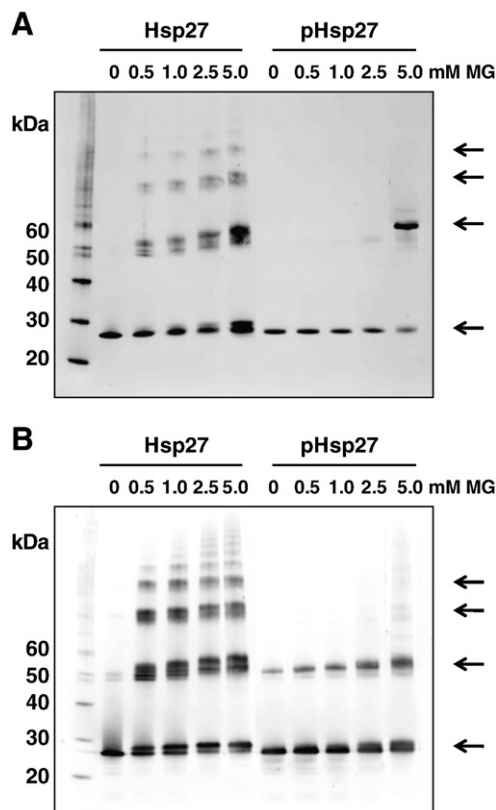

Fig. 3. Chemical modification of Hsp27 by MG. MG-modified Hsp27 and MG-modified phosphorylated Hsp27 were identified by immunoblot analysis using antibodies to argpyrimidine (A) or Hsp27 (B).
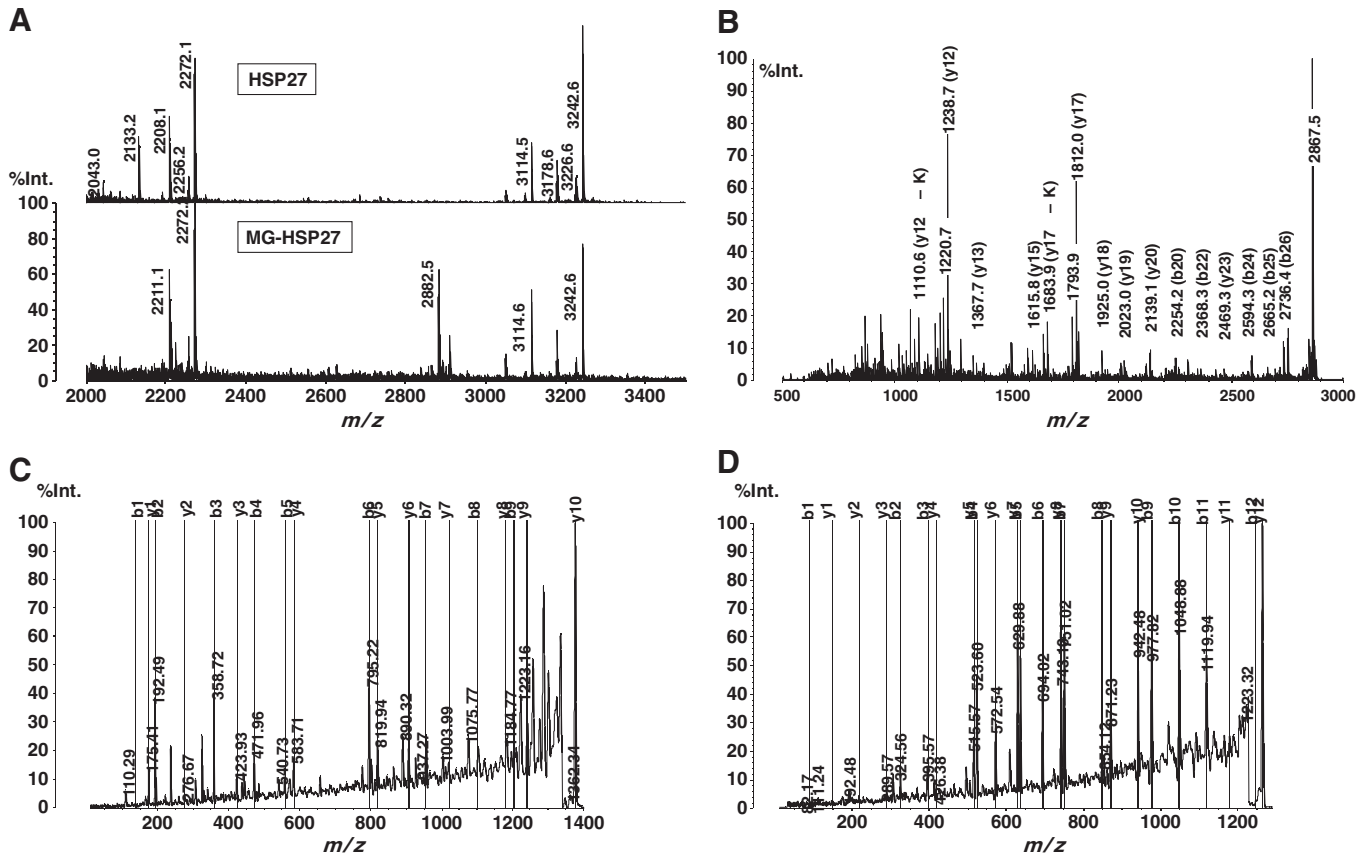
Fig. 4. MALDI-MS analyses of peptides from Hsp27 and MG-Hsp27. MS spectra of trypsin-digested native control Hsp27 and MG-modified Hsp27 (MG-Hsp27) peptides (A). MALDI-MS/MS spectrum of $[M+H]^+$ ion at m/z 2882.5 from the MG-Hsp27 fragment digested with trypsin (B). MALDI-MS/MS spectrum of $[M+H]^+$ ions at m/z 1377.4 from the MG-Hsp27 fragment digested with both trypsin and V8 protease (C). MALDI-MS/MS spectrum of $[M+H]^+$ ions at m/z 1265.3 from the MG-Hsp27 fragment digested with both trypsin and V8 protease (D).

fuses directly with the plasma membrane and delivers the captured protein into the cells by endocytosis; endosomes then release the captured protein into the cytoplasm. The cells were incubated for up to 48 h after introductions of native Hsp27 and MG-Hsp27, and cell proliferation was measured by WST-8. The viability of RIE cells was unaffected by the introduction of either native Hsp27 or MG-Hsp27 (Fig. 5A). To determine the effects of native Hsp27 and MG-Hsp27 on apoptosis, the native unmodified Hsp27- and MG-Hsp27-introduced

Table 1
Peptides identified by MALDI-MS and LC-MALDI-TOF MS/MS analyses of enzymatic digests of MG-Hsp27. Modification sites are underlined.

Theoretical mass	Start	End	Sequence	Modifications	Enzyme
1041.25	5	12	RVPFSLLR	5-Hydro-5-methylimidazolone (R)	Trypsin
1556.76	28	40	LFDQAFGLPRLPE	5-Hydro-5-methylimidazolone (R)	Trypsin + V8
2738.01	41	64	EWSQWLGGSSWPGYVRPLPPAAIE	5-Hydro-5-methylimidazolone (R)	Trypsin + V8
1570.75	65	79	SPAVAAPAYSRALSR	5-Hydro-5-methylimidazolone (R)	Trypsin + V8
2412.61	65	87	SPAVAAPAYSRALSRQLSSGVSE	2× 5-Hydro-5-methylimidazolone (R)	Trypsin + V8
1318.44	88	96	IRHTADRWR	2× 5-Hydro-5-methylimidazolone (R)	Trypsin + V8
2180.42	95	112	WRVSLDVNHFAPDELTVK	5-Hydro-5-methylimidazolone (R)	Trypsin
1769.91	113	127	TKDGVVEITGKHEER	Carboxyethyllysine (K)	Trypsin
2856.02	113	136	TKDGVVEITGKHEERQDEHGYISR	Carboxyethyllysine (K)	Trypsin
1540.63	115	127	DGVVEITGKHEER	Carboxyethyllysine (K)	Trypsin
2626.75	115	136	DGVVEITGKHEERQDEHGYISR	Carboxyethyllysine (K)	Trypsin
2680.79	115	136	DGVVEITGKHEERQDEHGYISR	5-Hydro-5-methylimidazolone (R); carboxyethyllysine (K)	Trypsin
1709.73	124	136	HEERQDEHGYISR	5-Hydro-5-methylimidazolone (R)	Trypsin
2274.39	124	140	HEERQDEHGYISRCFTR	5-Hydro-5-methylimidazolone (R)	Trypsin
1722.84	128	140	QDEHGYISRCFTR	5-Hydro-5-methylimidazolone (R)	Trypsin
1350.5	131	140	HGYISRCFTR	5-Hydro-5-methylimidazolone (R)	Trypsin + V8
1376.54	131	140	HGYISRCFTR	Argpyrimidine (R)	Trypsin + V8
1532.72	131	141	HGYISRCFTRK	2× 5-Hydro-5-methylimidazolone (R)	Trypsin + V8
2883.17	172	198	LATQSNEITIPVTFESRAQLGGPEAAK	5-Hydro-5-methylimidazolone (R)	Trypsin
1238.35	187	198	SRAQLGGPEAAK	5-Hydro-5-methylimidazolone (R)	Trypsin + V8
1256.37	187	198	SRAQLGGPEAAK	Dihydroxyimidazolidine (R)	Trypsin + V8
1264.39	187	198	SRAQLGGPEAAK	Argpyrimidine (R)	Trypsin + V8

Table 2
Peptides identified by MALDI-MS and LC-MALDI-TOF MS/MS analyses of enzymatic digests of MG-modified phosphorylated Hsp27. Modification sites are underlined.

Theoretical mass	Start	End	Sequence	Modifications	Enzyme
1041.01	13	20	GPSWDPFR	Phospho (S)	Trypsin + V8
1041.01	13	20	GPSWDPFR	Phospho (S)	Trypsin
1039.98	21	27	DWYPHSR	Phospho (S)	Trypsin
1169.18	65	75	SPAVAAPAYSR	Phospho (S)	Trypsin + V8
1650.73	65	79	SPAVAAPAYSRALSR	Phospho (S); 5-hydro-5-methylimidazolone (R)	Trypsin + V8
1668.74	65	79	SPAVAAPAYSRALSR	Phospho (S); dihydroxyimidazolidine (R)	Trypsin + V8
1155.15	80	89	QLSSGVSEIR	Phospho (S)	Trypsin
1789.8	80	94	QLSSGVSEIRHTADR	Phospho (S); 5-hydro-5-methylimidazolone (R)	Trypsin
922	88	94	IRHTADR	5-Hydro-5-methylimidazolone (R)	Trypsin + V8
1318.44	88	96	IRHTADRWR	2× 5-Hydro-5-methylimidazolone (R)	Trypsin + V8
995.05	90	96	HTADRWR	5-Hydro-5-methylimidazolone (R)	Trypsin + V8
995.05	90	96	HTADRWR	5-Hydro-5-methylimidazolone (R)	Trypsin
1769.91	113	127	TKDGVVEITGKHEER	Carboxyethyllysine (K)	Trypsin
1841.97	113	127	TKDGVVEITGKHEER	2× Carboxyethyllysine (K)	Trypsin
1540.63	115	127	DGVVEITGKHEER	Carboxyethyllysine (K)	Trypsin
1041.12	120	127	ITGKHEER	Carboxyethyllysine (K)	Trypsin + V8
1709.73	124	136	HEERQDEHGYISR	5-Hydro-5-methylimidazolone (R)	Trypsin
1722.84	128	140	QDEHGYISRCFTR	5-Hydro-5-methylimidazolone (R)	Trypsin
1350.5	131	140	HGYISRCFTR	5-Hydro-5-methylimidazolone (R)	Trypsin + V8
1532.72	131	141	HGYISRCFTRK	2× 5-Hydro-5-methylimidazolone (R)	Trypsin + V8
968.02	187	195	SRAQLGGPE	5-Hydro-5-methylimidazolone (R)	Trypsin + V8
1238.35	187	198	SRAQLGGPEAAK	5-Hydro-5-methylimidazolone (R)	Trypsin + V8
1256.37	187	198	SRAQLGGPEAAK	Dihydroxyimidazolidine (R)	Trypsin + V8

cells were cultured in 6-well plates and then treated with H_2O_2 (0.1, 0.5 and 1.0 mM). Exposure to 1.0 mM hydrogen peroxide led to necrosis. The intracellular delivery of native Hsp27 and MG-Hsp27 to RIE cells was examined by Western blot analysis (Fig. 5B). The density of Hsp27 band was quantified by CS Analyzer—Image Analysis Software. The ratio of band density of Hsp27 to band density of tubulin was calculated. Native Hsp27 and MG-Hsp27 intracellular delivery to RIE cells were 1.77 and 1.53, respectively. The treatment of Hsp27- and MG-Hsp27-introduced cells with hydrogen peroxide did not affect Hsp27 protein abundances. The same levels of Hsp27 and MG-Hsp27 were observed after treatment with hydrogen peroxide. The apoptotic RIE cells were assayed by flow cytometry using FITC-Annexin V binding and PI staining. Fig. 5C shows that 0.1 mM hydrogen peroxide treatment results in an increase in FITC-Annexin V-positive cells. The introduction of native Hsp27 decreased the number of FITC-Annexin V positive cells induced by hydrogen peroxide. The transfer of MG-Hsp27 into the cells dramatically reduced the number of FITC-Annexin V positive cells. These results suggest that the introduction of native Hsp27 delays the induction of apoptosis, and the MG modification of Hsp27 completely inhibits the induction of apoptosis.

The efficacy of MG modification of Hsp27 on hydrogen peroxide-induced intracellular ROS formation was evaluated. Native Hsp27, pHsp27, MG-Hsp27 or MG-pHsp27 was introduced into RIE cells with BioPORTER. To detect ROS, we used 2-[6-(4′-amino)phenoxy-3H-xanthen-3-on-9-yl] benzoic acid (APF). APF can detect hydroxyl radicals (·OH) and is completely resistant to autoxidation, both *in vitro* and *in vivo*[17]. Hydrogen peroxide treatment caused an increase in the amount of intracellular ·OH of BioPORTER-treated control RIE cells in a concentration-dependent manner (Fig. 6A). The introduction of MG-Hsp27 prevented ·OH generation in the cells treated with 0.1 mM hydrogen peroxide compared with the introduction of native Hsp27 or the BioPORTER-treated controls.

It is known that the formation of large oligomeric Hsp27 prevents cytochrome *c*-mediated caspase activation [16], so we examined whether MG modification affected the regulation of caspase activation by Hsp27 using a cell-free system. The addition of cytochrome *c* and dATP to extracts from BioPORTER-treated control RIE cells resulted in the activation of caspase-3 and caspase-9 (Fig. 6B). Extracts from MG-pHsp27-introduced cells inhibited the activation of caspase-3,

whereas no inhibition was observed by using extracts from native Hsp27- or pHsp27-introduced cells. Caspase-9 activation was inhibited by the introduction of all Hsp27 moieties (Hsp27, MG-Hsp27, pHsp27, and MG-pHsp27; $p < 0.01$ versus BioPORTER-treated control cells). MG modification did not affect the inhibition of caspase-9 activation by Hsp27. The introduction of pHsp27 was less effective in inhibiting caspase-9 activation, but this inhibitory effect of pHsp27 was enhanced by MG modification. These results suggested that MG modification of pHsp27 potentiate the suppression of cytochrome *c*-mediated caspase activation.

We also determined whether Hsp27 introduction exerts a protective effect against caspase activation during hydrogen peroxide-induced apoptotic cell death. In BioPORTER-treated control RIE cells, both caspase-3 and caspase-9 were activated by treatment with 0.1 mM hydrogen peroxide. The introduction of Hsp27 into RIE cells prevented both caspase-3 and caspase-9 activation, as shown in Fig. 6C. MG modification enhanced the inhibitory effect of Hsp27 on caspase-3 ($p < 0.01$ versus Hsp27-introduced cells) and caspase-9 ($p < 0.001$ versus Hsp27-introduced cells) activations. Phosphorylation of Hsp27 resulted in the loss of this effect. MG modification of pHsp27 increased the inhibitory effects of both caspase-3 and caspase-9 activations, but the overall effect was still less than that seen with Hsp27. These results indicate that MG modification is essential for conferring protection against caspase-mediated apoptosis induced by hydrogen peroxide.

3.4. Intracellular levels of lactate, the principal end-product of MG metabolism

It is difficult to measure intracellular levels of MG directly because of its high reactivity. MG reacts rapidly with guanidine group such as arginine residue [12]. The glyoxalase system, comprising the metalloenzymes glyoxalase I and glyoxalase II, is an almost universal metabolic pathway involved in the detoxification of the glycolytic byproduct MG to D-lactate. Production of lactate in RGM-1 and RGK-1 cells was measured by using D-lactate and L-lactate dehydrogenase-based assays (Fig. 8). The level of D-lactate in RGK-1 cells was found to be significantly higher compared with that in RGM-1 cells (2-fold, $p < 0.05$). The intracellular D-lactate contents of RGM-1 and RGK-1 cells were 0.06 ± 0.01 and 0.13 ± 0.01 mM/mg of cell lysate protein, respectively. Moreover, the contents of L-lactate of RGM-1 and RGK-1
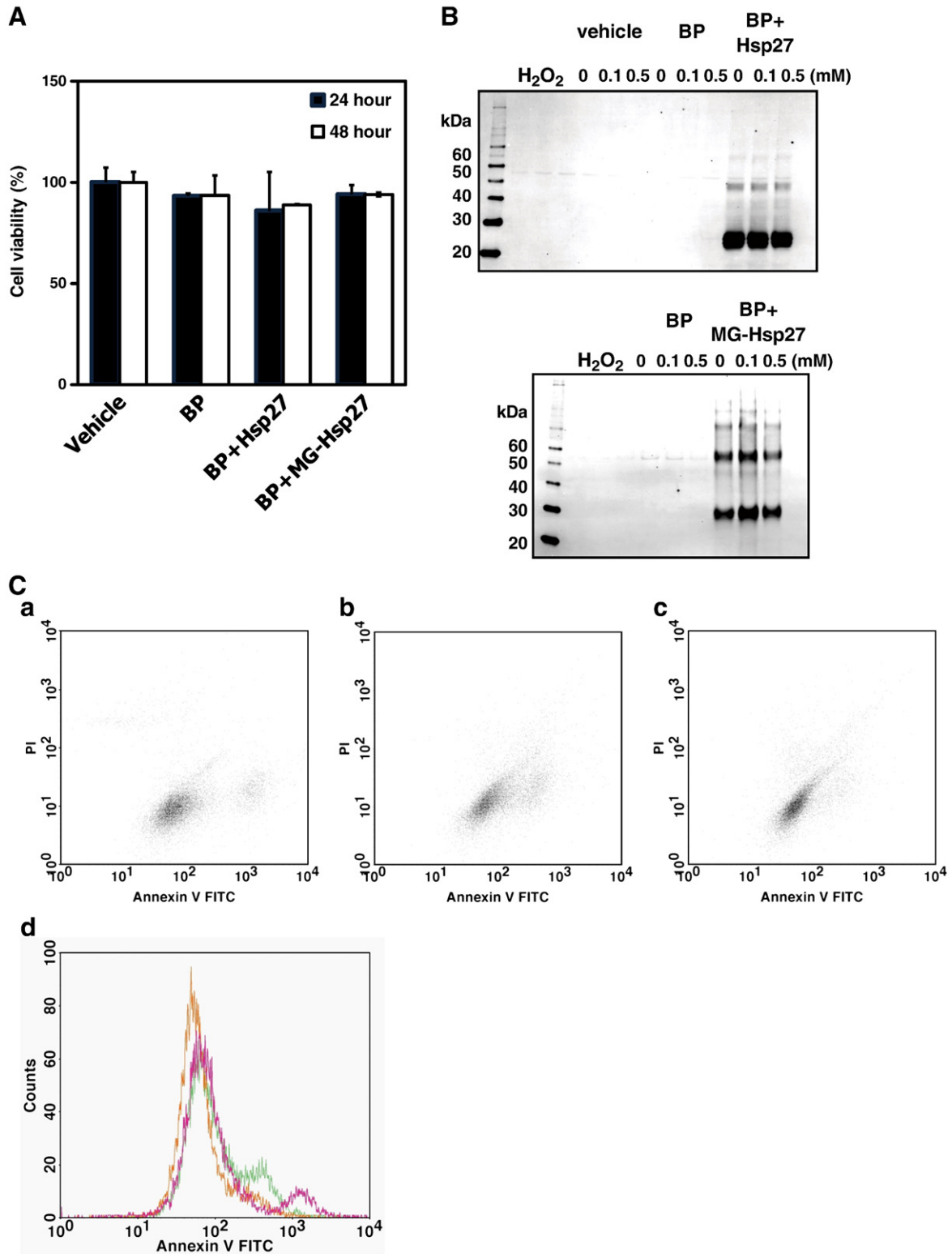
A

B

C

Fig. 5. Effect of MG modification of Hsp27 on hydrogen peroxide-induced apoptosis. Native Hsp27, or MG-Hsp27, was introduced into RIE cells with BioPORTER. After incubation for 24 and 48 h at 37 °C, the effect of Hsp27 on cell viability was assessed by WST-8 (A). After a 4-h incubation, apoptosis was induced by treating the cells with hydrogen peroxide for 24 h. The introductions of native Hsp27 and MG-Hsp27 were assessed by Western blot analysis (B). After treating cells with hydrogen peroxide for 24 h, cell extracts from Hsp27- and MG-Hsp27-introduced cells were examined. The extent of apoptosis in RIE cells was assayed by FACS (FITC-Annexin V binding and PI staining) (a) BioPORTER-treated cells, (b) Hsp27-introduced cells, (c) MG-Hsp27-introduced cells, (d) apoptosis analyzed by FITC-Annexin V binding (red: BioPORTER, green: BioPORTER + Hsp27, orange: BioPORTER + MG-Hsp27) (C).

cells were 0.32 ± 0.01 and 0.77 ± 0.01 mM/mg of cell lysate protein, respectively. The level of L-lactate in RGK-1 cells was 2.4 times higher than that in RGM-1 cells ($p < 0.00001$). In RGK-1 and RGM-1 cells, the concentration of D-lactate was one-sixth and one-fifth of

concentration of L-lactate, respectively. The total lactate content in RGK-1 cells was 0.90 ± 0.08 mM/mg of cell lysate protein, while that in RGM-1 cells was 0.38 ± 0.07 mM/mg of cell lysate protein. These results support high levels of lactate in cancer cells.
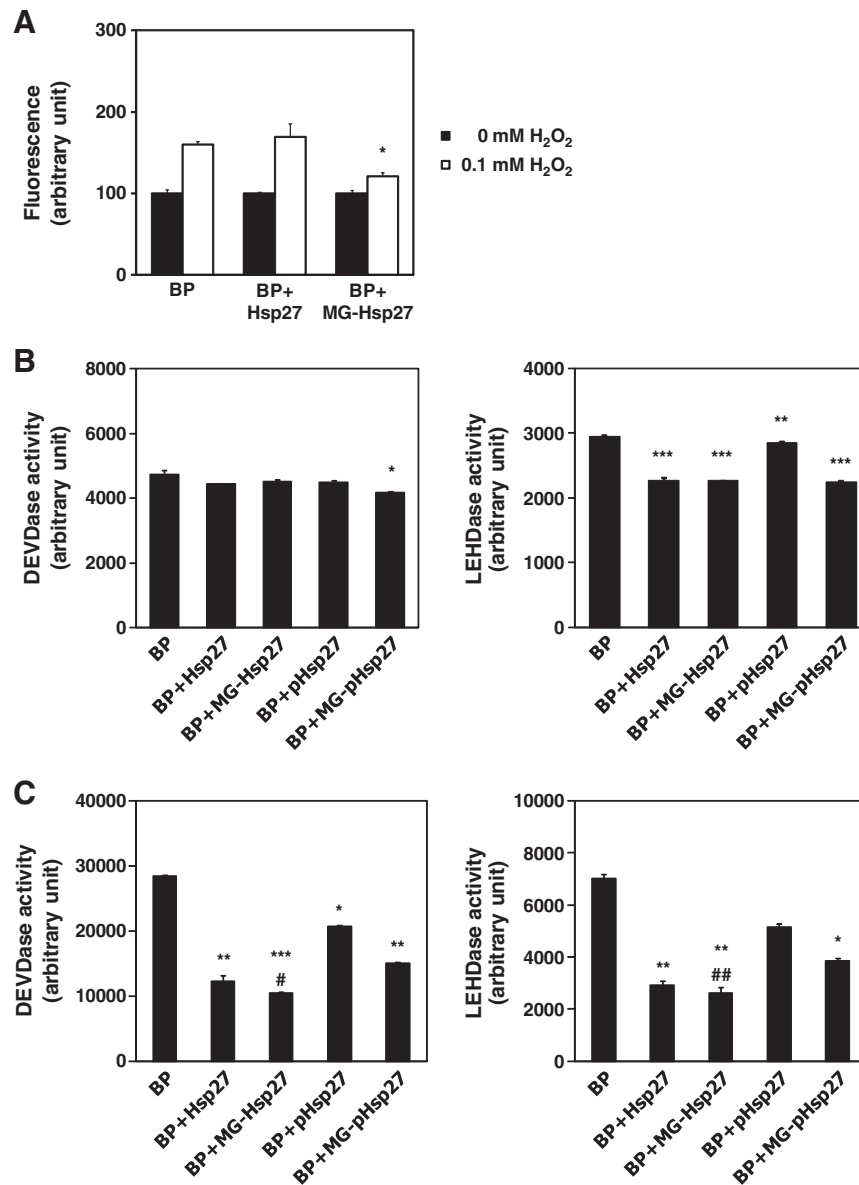
Fig. 6. Effects of MG modification of Hsp27 on hydrogen peroxide-induced intracellular ROS formation and on caspase activation in RIE cells. Native Hsp27, phosphorylated Hsp27 (pHsp27), MG-Hsp27 or MG-pHsp27 was introduced into RIE cells with BioPORTER. ROS formation was induced by treating the cells with 0.1 mM hydrogen peroxide (A). Intracellular ROS formation was detected with a fluorescent probe, APF. The vertical bars represent SEM values of triplicate determinations. $*p<0.05$ versus BioPORTER-treated control cells. Caspase activation was mediated by cytochrome c (B). Cell-free extracts from each RIE cells were treated with 10 μM cytochrome c and 1 mM dATP for 30 min. Caspase-3 and caspase-9 activities were assessed by measuring the cleavage of the DEVD-AFC and LEHD-AFC substrates, respectively. $**p<0.01$ and $***p<0.001$ versus BioPORTER-treated control cells. Caspase activation was induced by treating the cells with 0.1 mM hydrogen peroxide (C). $^{\#}p<0.01$ and $^{\#\#}p<0.001$ versus Hsp27-introduced cells.

4. Discussion

In this study, we identified a link between posttranslational modification and carcinogenesis. Rat Hsp25 and human Hsp27 were identified as one of the major MG-modified proteins in gastrointestinal cancer. Hsp27 is human homolog of rodent Hsp25 [15]. The modification of Hsp25 by MG was not seen in non-carcinogenetic RGM-1 cells, RIE cells or YAMC cells. Immunoprecipitation studies with anti-Hsp25/Hsp27 antibodies demonstrated that MG modification of Hsp25/Hsp27 is associated with cancer development.

In normal cells, Hsp27 participates in cytoskeletal, redox state and protein folding homeostasis. It is also involved in the protection of cells against stress. Hsp27 has beneficial effects on protein conformation and in inflammation-related diseases. High levels of constitutive Hsp27 expression have been detected in several cancer cells, particularly carcinomas [18,19]. Recently, the number of reports

dealing with Hsp27 in cancer pathology has grown exponentially. Moreover, experiments in rodents have highlighted the tumorigenic potential of Hsp27 expression [20]. Hsp27 is thought to increase the ability of some cancer cells to resist and to evade the apoptotic processes mediated by the immune system. In the current study, no noticeable differences in expression level of Hsp25/Hsp27 between noncancerous and cancerous cells were found. Additionally, MG modification was detected in only cancerous cells. It is expected that MG modification regulates the apoptotic processes. In future studies, to explore the relationship between MG modification and carcinogenesis, LC-MALDI analysis of MG-modified Hsp27 in clinical sample should be considered.

Recently, argpyrimidine formation in Hsp27 has been identified in human non-small-cell lung carcinoma cells [3]. It has been uncertain whether the concentration of MG is higher in gastrointestinal cancer cells than in normal cells. It is difficult to measure directly MG because
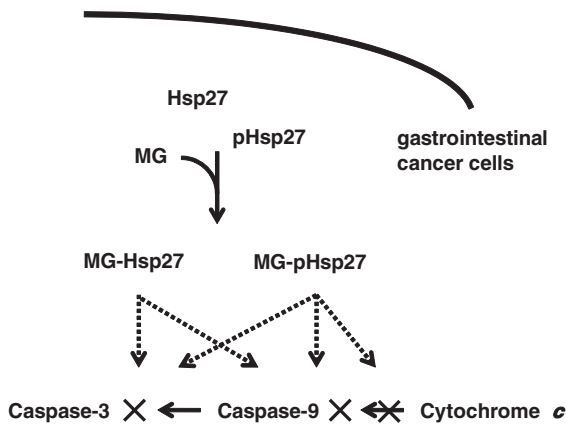
Fig. 7. A proposed mechanism for prevention of caspase activation by Hsp27. MG modification in gastrointestinal cancer cells promotes Hsp27 and pHsp27 properties.

of its high reactivity. Gluconeogenesis occurs without ATP consumption through the MG pathway when used as a substrate of ketone bodies via the pathway: butyric acid (butyrate) → beta-hydroxybutyrate → acetoacetate → acetone → acetol → methylglyoxal →S-D-lactol-glutathione → D -lactate → pyruvate → D-lactate [21]. It has previously been reported that pyruvate concentration is significantly lower in colon tumors than in normal tissue, and slightly lower in stomach tumors, whereas lactate concentration in tumor tissues is higher in both tumor types than in normal tissue [2]. We measured the levels of intracellular lactate which is the end molecule of the MG pathway because MG is difficult to measure directly. Indeed, the total lactate content in MNNG-induced mutant of RGM-1 gastric epithelial cell line, which is named RGK-1 cells, was dramatically higher than that in RGM-1 cells (Fig. 8). This clearly indicates that cancer cells are highly dependent on anaerobic breakdown of pyruvate. High lactate dehydrogenase-5 activity, and the resulting increase in conversion of pyruvate to lactate has been identified in colon cancer [22,23]. Active glycolysis also increases the cytosolic $NADH/NAD^+$ ratio, thereby increasing the activity of lactate dehydrogenase [24]. Enhanced pyruvate-to-lactate conversion may also be due to the activation of the pyruvate dehydrogenase kinase, isozyme 1 (PDK1), in cancer cells, which inactivates pyruvate dehydrogenase and leads to the inactivation of the TCA cycle [25]. Therefore, it is likely that cancer cells preferentially use glucose because of intrinsic metabolic characteristics, and micro-environmental factors such as hypoxia. Moreover, the MG pathway represents an energetically unfavorable bypass to the glycolytic reactions of the lower Embden–Meyerhof–Parnas pathway using pyruvate [26,27]. Activation of the MG pathway has been confirmed when the intracellular uptake of glucose 6-phosphate or other carbon substrates such as xylose, lactose, arabinose, glycerol or gluconate are deregulated by mutation and/or by addition of cAMP
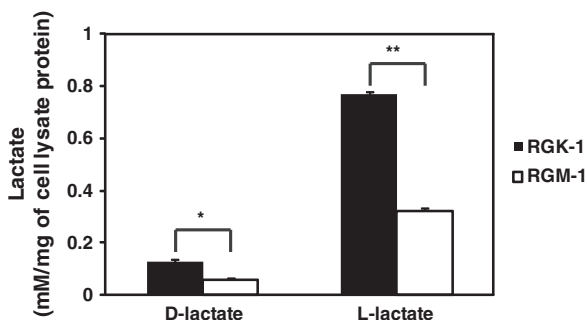

Fig. 8. Contents of D-lactate and L-lactate in RGK-1 cells and RGM-1 cells. Intracellular lactate levels were estimated by D-lactate and L-lactate dehydrogenase-based assays. $*p < 0.05$ and $**p < 0.00001$ versus RGM-1 cells.

[28–30]. Moreover, the extremely low glucose content in tumor tissues might result from both a poor blood supply and the high glucose consumption by cancer cells. In addition, the glyoxalase pathway catalyzes the formation of lactate from MG in the presence of glutathione. D-lactate is produced in the MG pathway as the end-product of glyoxalase II enzymatic reaction. The intracellular D-lactate concentration in RGK-1 cells was twice as high as that in RGM-1 cells ($p < 0.05$). There is an increase in the flux of MG metabolized to lactate via the glyoxalase pathway with high glucose concentrations [31]. RGK-1 cells are the first MNNG-induced neoplastic mutant cells derived from a noncancerous, nonembryonic gastric epithelial cell line. Ultrastructural results show homogenous, dense secretory granules and deformed mitochondria in RGK-1 cells [10]. RGM-1 cells have no secretory granules, normal-shaped mitochondria, and abundant polyribosomes. Moreover, mutant RGK-1 cells have shown tumorigenic potential in all mice into which they have been injected [10]. We consider that the intracellular accumulation of MG is implicated in the pathogenesis of cancer in RGK-1 cells. It is important to determine whether high MG modification promotes the development of cancer. Because the intracellular MG concentration is regulated by glyoxalase, the experiments of overexpression or knockdown of glyoxalase should be done in the future.

The large oligomers of Hsp27, which bear chaperone-like activity, are also responsible for the tumorigenic activity of Hsp27 [32]. Therefore, it cannot be excluded that large Hsp27 oligomers may act in a manner similar to Hsp90, and bind specific client proteins that participate in the tumorigenic and metastatic processes. In this study, numerous post-translational modifications of Hsp25/Hsp27 in a large number of cancer cells were found. Recombinant Hsp27 and phosphorylated Hsp27 were polymerized during incubation with MG in vitro. Moreover, large MG-modified Hsp27 and MG-modified pHsp27 oligomers were detected in tumorigenic HT-29 cells. It is suggested that the polymerizations of Hsp27 and pHsp27 are promoted by modification of MG. In Fig. 3, cross-linked Hsp27 and pHsp27 increased with increasing concentration of MG. Previous research has demonstrated that chaperone-like activity of Hsp27, even pHsp27, is greatly facilitated by MG modification [9]. Additionally, Hsp modification by MG enhances the hydrophobicity [33]. The chaperone function of alpha-crystallin is attributed to hydrophobic regions of the protein, and modification by low concentration of MG increases its hydrophobicity [33]. Hsp27 also has hydrophobic N-terminal region that contributes to its oligomerization [34]. An increased molecular chaperone function in cancer cells is likely related to oligomerization of Hsp27 by MG modification and an increased hydrophobicity. Future studies will investigate the effect of MG modification on chaperone function in cancer cells.

The formation of argpyrimidine on Hsp27 has also been identified in endothelial cells [35], lens epithelial cells [9] and rat kidney mesangial cells [36], indicating that Hsp27 is a protein highly susceptible to MG modification. MALDI-MS/MS analysis of the peptide fragments derived from recombinant human Hsp27 showed MG modification sites at Arg-5, Arg-96, Arg-127, Arg-136, Arg-188, and Lys-123. For the first time, we confirmed the formation of argpyrimidine on trypsin- and V8 protease-digested fragments of MG-modified Hsp27 by LC-MALDI-TOF MS/MS analysis. However, we failed to detect argpyrimidine adducts in the peptide fragments derived from MG-modified phosphorylated Hsp27. It is unclear whether MG is insensitive to pHsp27 or whether the peptide fragments derived from MG-pHsp27 are beyond the limit of detection. The upper limit of detectable mass range is approximately 35,000 Da. At least immunoreactivity against argpyrimidine was observed with polymerized MG-pHsp27 in our experiments. Meanwhile, it has been shown that MG forms a number of adducts with lysine residues in polymerized proteins. Nagaraj et al. [33] have described an imidazolium cross-link structure, imidazolysine. In this study, because the antibody does not recognize imidazolysine [12], this structure was not

searched in the data base of LC-MALDI-TOF MS/MS analyses. It is predicted that imidazolium cross-link structures are generated in MG-modified Hsp27.

As described previously, Hsp27 is expressed throughout the body and plays an important role in cellular functions such as apoptosis [9] and actin polymerization [37–39]. In stressed cells, increased levels of Hsp27 facilitate the repair, or destruction, of damaged proteins, thus promoting cell recovery. In our previous study, we found that Hsp27 shows increased anti-apoptotic effects in lens epithelial cells after modification by MG, which is due to multiple mechanisms including the enhancement of chaperone function, and inhibition of caspase activity [9,33,40]. The transfer of MG-modified Hsp27 significantly inhibits staurosporine-induced apoptotic cell death and ROS production in a human lens epithelial cell line (HLE B-3) [9]. In this study, RIE cells also exhibited enhanced anti-apoptotic property by MG modification of Hsp27. In particular, MG modification of Arg-188 in Hsp27 is essential for inhibiting cytochrome c-mediated caspase activation in 293T cells transfected with mutant of Hsp27 (Arg-188 to glycine) [41]. MALDI-MS/MS analysis of the peptide fragments derived from MG-modified Hsp27 showed that Arg-188 is susceptible to modification. YAMC cells expressed Hsp25 by treatment with butyrate were not resistant to hydrogen peroxide-induced apoptosis (data not shown). Additionally, we found that the expression levels of Hsp25 showed no difference between RGM-1 cells and mutant RGK-1 cells. Our experiments, especially immunoprecipitation assays, showed that the expressed Hsp25 in RIE cells and YAMC cells by treatment with butyrate was not modified by MG, whereas Hsp25 in mutant RGK-1 cells and Hsp27 in HT-29 cells and in ascending colon and rectum of patient with adenoma and advanced cancer were. These results suggest that MG modification of Arg-188 in Hsp25/Hsp27 plays a key role in the development of cancer. It was impossible to detect MG modification of Arg-188 in protein extracts from cultured cells and clinical samples by MALDI-MS analysis due to low expression level. Future studies are needed to confirm the effect of Arg-188 in Hsp25/Hsp27 in cancer cells.

It has been speculated that MG may protect cells against hyperglycemia-induced damage in diabetes because MG modification of Hsp27 enhances its chaperone function, as has been shown for alpha-crystallin [9,33]. However, protein-modifying sugars and ascorbic acid have no such effect and actually reduce chaperone function [33]. Thus, it is believed that MG modification of Hsp27 is different from other glycation. Additionally, a study in human lens epithelial cells indicated that MG modification enhances the binding of Hsp27 to cytochrome c and, subsequently, the protection from caspase-3 dependent cell death [9]. Our experiments showed that the transfer of Hsp27 using a cationic lipid inhibits the hydrogen-peroxide-induced apoptosis in the RIE cell line and that MG modification of Hsp27 enhances this inhibition. The introduction of MG-Hsp27 reduced intracellular ROS generation also. MG-modified Hsp27 showed no difference in proliferation of rat intestinal epithelial cell line compared to other controls (Hsp27, vehicle, and BP-treatment). When apoptosis was mediated by the addition of both cytochrome c and ATP to the cell-free cytosol, the inhibition of caspase-3 activation by phosphorylated Hsp27, and of caspase-9 activation by both native and phosphorylated Hsp27, was enhanced by MG modification. This shows that MG modification of pHsp27 prevents the activations of both caspase-3 and caspase-9 induced by the release of cytosolic cytochrome c from mitochondria. Moreover, MG modification of native Hsp27 and phosphorylated Hsp27 inhibited the activations of both caspase-3 and caspase-9 during oxidant-induced cell death. These results suggest that Hsp27 reacts immediately with MG and serves protective functions against caspase activation in gastrointestinal cancer cells (Fig. 7). The enhanced inhibitory effects of MG modification on caspase activation are similar to those seen for chaperone activity [9]. We propose that MG modification of Hsp27 can protect against caspase-3 and caspase-9 activations without affecting the rate of cytochrome c release and promote cell survival.

Almost all phosphorylated Hsp27 were modified by MG in lens epithelial cells [9] and in HT-29 cells. Thus, while MG modification of Hsp27 can maintain transparency and protect against apoptosis in lens cells which has a slow turnover rate, this modification may be involved in the pathogenesis of cancer in the gastrointestinal epithelium which has a rapid turnover rate.

In conclusion, the specific immunoreactivity against the MG-modified protein was observed in gastrointestinal carcinoma cell lines and in ascending colon and rectum of patients with cancer, but not in normal subjects. We identified this modified protein as Hsp25/Hsp27 and showed for the first time that argpyrimidine adducts are generated at Arg-136 and Arg-188 of MG-modified Hsp27, which is thought to be necessary for its enhanced anti-apoptotic effects. Furthermore, we found that MG-modified Hsp27 effectively inhibits caspase activation, ROS production, and the induction of apoptosis in hydrogen peroxide-treated cells. Therefore, our results suggest that posttranslational modification of Hsp27 by MG may contribute to the development of gastrointestinal cancer.

References

[1] O. Warburg, On the origin of cancer cells, Science 123 (1956) 309–314.
[2] A. Hirayama, K. Kami, M. Sugimoto, M. Sugawara, N. Toki, H. Onozuka, T. Kinoshita, N. Saito, A. Ochiai, M. Tomita, H. Esumi, T. Soga, Quantitative metabolome profiling of colon and stomach cancer microenvironment by capillary electrophoresis time-of-flight mass spectrometry, Cancer Res. 69 (2009) 4918–4925.
[3] J.W. van Heijst, H.W. Niessen, R.J. Musters, V.W. van Hinsbergh, K. Hoekman, C.G. Schalkwijk, Argpyrimidine-modified heat shock protein 27 in human non-small cell lung cancer: a possible mechanism for evasion of apoptosis, Cancer Lett. 241 (2006) 309–319.
[4] A.P. Arrigo, S. Simon, B. Gibert, C. Kretz-Remy, A. Nivon, A. Czekalla, D. Guillet, M. Moulin, C. Diaz-Latoud, P. Vicart, Hsp27 (HspB1) and alphaB-crystallin (HspB5) as therapeutic targets, FEBS Lett. 581 (2007) 3665–3674.
[5] H. Ren, M.W. Musch, K. Kojima, D. Boone, A. Ma, E.B. Chang, Short-chain fatty acids induce intestinal epithelial heat shock protein 25 expression in rats and IEC 18 cells, Gastroenterology 121 (2001) 631–639.
[6] C. Decroos, Y. Li, G. Bertho, Y. Frapart, D. Mansuy, J.L. Boucher, Oxidative and reductive metabolism of tris(p-carboxyltetrathiaaryl)methyl radicals by liver microsomes, Chem. Res. Toxicol. 22 (2009) 1342–1350.
[7] D. Stokoe, K. Engel, D.G. Campbell, P. Cohen, M. Gaestel, Identification of MAPKAP kinase 2 as a major enzyme responsible for the phosphorylation of the small mammalian heat shock proteins, FEBS Lett. 313 (1992) 307–313.
[8] J. Rouse, P. Cohen, S. Trigon, M. Morange, A. Alonso-Llamazares, D. Zamanillo, T. Hunt, A.R. Nebreda, A novel kinase cascade triggered by stress and heat shock that stimulates MAPKAP kinase-2 and phosphorylation of the small heat shock proteins, Cell 78 (1994) 1027–1037.
[9] T. Oya-Ito, B.F. Liu, R.H. Nagaraj, Effect of methylglyoxal modification and phosphorylation on the chaperone and anti-apoptotic properties of heat shock protein 27, J. Cell. Biochem. 99 (2006) 279–291.
[10] O. Shimokawa, H. Matsui, Y. Nagano, T. Kaneko, T. Shibahara, A. Nakahara, I. Hyodo, A. Yanaka, H.J. Majima, Y. Nakamura, Y. Matsuzaki, Neoplastic transformation and induction of H+, K+ −adenosine triphosphatase by N-methyl-N′-nitro-N-nitrosoguanidine in the gastric epithelial RGM-1 cell line, In Vitro Cell. Dev. Biol. Anim. 44 (2008) 26–30.

[11] R.B. Brandt, S.A. Siegel, M.G. Waters, M.H. Bloch, Spectrophotometric assay for D-(−)-lactate in plasma, Anal. Biochem. 102 (1980) 39–46.

[12] T. Oya, N. Hattori, Y. Mizuno, S. Miyata, S. Maeda, T. Osawa, K. Uchida, Methylglyoxal modification of protein. Chemical and immunochemical characterization of methylglyoxal–arginine adducts, J. Biol. Chem. 274 (1999) 18492–18502.

[13] E. Muller, W. Neuhofer, A. Ohno, S. Rucker, K. Thurau, F.X. Beck, Heat shock proteins HSP25, HSP60, HSP72, HSP73 in isoosmotic cortex and hyperosmotic medulla of rat kidney, Pflugers Arch. 431 (1996) 608–617.

[14] S. Gonin, N. Fabre-Jonca, C. Diaz-Latoud, J.P. Rouault, A.P. Arrigo, Transformation by T-antigen and other oncogenes delays Hsp25 accumulation in heat shocked NIH 3T3 fibroblasts, Cell Stress Chaperones 2 (1997) 238–251.

[15] T. Rogalla, M. Ehrnsperger, X. Preville, A. Kotlyarov, G. Lutsch, C. Ducasse, C. Paul, M. Wieske, A.P. Arrigo, J. Buchner, M. Gaestel, Regulation of Hsp27 oligomerization, chaperone function, and protective activity against oxidative stress/tumor necrosis factor alpha by phosphorylation, J. Biol. Chem. 274 (1999) 18947–18956.

[16] H. Lambert, S.J. Charette, A.F. Bernier, A. Guimond, J. Landry, HSP27 multimerization mediated by phosphorylation-sensitive intermolecular interactions at the amino terminus, J. Biol. Chem. 274 (1999) 9378–9385.

[17] K. Setsukinai, Y. Urano, K. Kakinuma, H.J. Majima, T. Nagano, Development of novel fluorescence probes that can reliably detect reactive oxygen species and distinguish specific species, J. Biol. Chem. 278 (2003) 3170–3175.

[18] D.R. Ciocca, S.K. Calderwood, Heat shock proteins in cancer: diagnostic, prognostic, predictive, and treatment implications, Cell Stress Chaperones 10 (2005) 86–103.

[19] S.K. Calderwood, M.A. Khaleque, D.B. Sawyer, D.R. Ciocca, Heat shock proteins in cancer: chaperones of tumorigenesis, Trends Biochem. Sci. 31 (2006) 164–172.

[20] C. Garrido, A. Fromentin, B. Bonnotte, N. Favre, M. Moutet, A.P. Arrigo, P. Mehlen, E. Solary, Heat shock protein 27 enhances the tumorigenicity of immunogenic rat colon carcinoma cell clones, Cancer Res. 58 (1998) 5495–5499.

[21] V.N. Titov, L.F. Dmitriev, V.A. Krylin, V.A. Dmitriev, Methylglyoxal—a test for impaired biological functions of exotrophy and endoecology, low glucose level in the cytosol and gluconeogenesis from fatty acids (a lecture), Klin. Lab. Diagn. (2010) 22–36.

[22] M.I. Koukourakis, A. Giatromanolaki, A. Polychronidis, C. Simopoulos, K.C. Gatter, A.L. Harris, E. Sivridis, Endogenous markers of hypoxia/anaerobic metabolism and anemia in primary colorectal cancer, Cancer Sci. 97 (2006) 582–588.

[23] R. Mazzanti, M. Solazzo, O. Fantappie, S. Elfering, P. Pantaleo, P. Bechi, F. Cianchi, A. Ettl, C. Giulivi, Differential expression proteomics of human colon cancer, Am. J. Physiol. Gastrointest. Liver Physiol. 290 (2006) G1329–G1338.

[24] J.M. Argiles, J. Azcon-Bieto, The metabolic environment of cancer, Mol. Cell. Biochem. 81 (1988) 3–17.

[25] J.G. Pan, T.W. Mak, Metabolic targeting as an anticancer strategy: dawn of a new era? Sci. STKE 2007 (2007) e14.

[26] R.A. Cooper, A. Anderson, The formation and catabolism of methylglyoxal during glycolysis in *Escherichia coli*, FEBS Lett. 11 (1970) 273–276.

[27] Y. Kondoh, M. Kawase, Y. Kawakami, S. Ohmori, Concentrations of D-lactate and its related metabolic intermediates in liver, blood, and muscle of diabetic and starved rats, Res. Exp. Med. (Berl.) 192 (1992) 407–414.

[28] R.S. Ackerman, N.R. Cozzarelli, W. Epstein, Accumulation of toxic concentrations of methylglyoxal by wild-type *Escherichia coli* K-12, J. Bacteriol. 119 (1974) 357–362.

[29] R. Puskas, N. Fredd, C. Gazdar, A. Peterkofsky, Methylglyoxal-mediated growth inhibition in an *Escherichia coli* cAMP receptor protein mutant, Arch. Biochem. Biophys. 223 (1983) 503–513.

[30] R.J. Kadner, G.P. Murphy, C.M. Stephens, Two mechanisms for growth inhibition by elevated transport of sugar phosphates in *Escherichia coli*, J. Gen. Microbiol. 138 (1992) 2007–2014.

[31] P.J. Thornalley, Modification of the glyoxalase system in human red blood cells by glucose in vitro, Biochem. J. 254 (1988) 751–755.

[32] J.M. Bruey, C. Paul, A. Fromentin, S. Hilpert, A.P. Arrigo, E. Solary, C. Garrido, Differential regulation of HSP27 oligomerization in tumor cells grown in vitro and in vivo, Oncogene 19 (2000) 4855–4863.

[33] R.H. Nagaraj, T. Oya-Ito, P.S. Padayatti, R. Kumar, S. Mehta, K. West, B. Levison, J. Sun, J.W. Crabb, A.K. Padival, Enhancement of chaperone function of alpha-crystallin by methylglyoxal modification, Biochemistry 42 (2003) 10746–10755.

[34] S. Dai, Y. Jia, S.L. Wu, J.S. Isenberg, L.A. Ridnour, R.W. Bandle, D.A. Wink, D.D. Roberts, B.L. Karger, Comprehensive characterization of heat shock protein 27 phosphorylation in human endothelial cells stimulated by the microbial dithiole thiolutin, J. Proteome Res. 7 (2008) 4384–4395.

[35] C.G. Schalkwijk, J. van Bezu, R.C. van der Schors, K. Uchida, C.D. Stehouwer, V.W. van Hinsbergh, Heat-shock protein 27 is a major methylglyoxal-modified protein in endothelial cells, FEBS Lett. 580 (2006) 1565–1570.

[36] A.K. Padival, J.W. Crabb, R.H. Nagaraj, Methylglyoxal modifies heat shock protein 27 in glomerular mesangial cells, FEBS Lett. 551 (2003) 113–118.

[37] P. Negre-Aminou, R.E. van Leeuwen, G.C. van Thiel, P. van den Ijssel, W.W. de Jong, R.A. Quinlan, L.H. Cohen, Differential effect of simvastatin on activation of Rac(1) vs. activation of the heat shock protein 27-mediated pathway upon oxidative stress, in human smooth muscle cells, Biochem. Pharmacol. 64 (2002) 1483–1491.

[38] J. Huot, F. Houle, S. Rousseau, R.G. Deschesnes, G.M. Shah, J. Landry, SAPK2/p38-dependent F-actin reorganization regulates early membrane blebbing during stress-induced apoptosis, J. Cell Biol. 143 (1998) 1361–1373.

[39] J.H. Lee, D. Sun, K.J. Cho, M.S. Kim, M.H. Hong, I.K. Kim, J.S. Lee, Overexpression of human 27 kDa heat shock protein in laryngeal cancer cells confers chemoresistance associated with cell growth delay, J. Cancer Res. Clin. Oncol. 133 (2007) 37–46.

[40] A. Biswas, A. Miller, T. Oya-Ito, P. Santhoshkumar, M. Bhat, R.H. Nagaraj, Effect of site-directed mutagenesis of methylglyoxal-modifiable arginine residues on the structure and chaperone function of human alphaA-crystallin, Biochemistry 45 (2006) 4569–4577.

[41] H. Sakamoto, T. Mashima, K. Yamamoto, T. Tsuruo, Modulation of heat-shock protein 27 (Hsp27) anti-apoptotic activity by methylglyoxal modification, J. Biol. Chem. 277 (2002) 45770–45775.